Monitoring of a Peanut-shaped TBM Launching Shaft Excavation using Fibre Optics and Remote Sensing Techniques

I Li[1*], E H Y Sze[1], F L C Lo[1], S Q Lin[2], D Y Tan[2], A Y F Leung[2], A W Y Chan[3], T C W Wong[3], E Y M Chan[3]

[1]Geotechnical Engineering Office, Civil Engineering and Development Department, Hong Kong SAR, China
[2]The Hong Kong Polytechnic University, Hong Kong SAR, China
[3]East Development Office, Civil Engineering and Development Department, Hong Kong SAR, China

*Corresponding author
doi: https://doi.org/10.21467/proceedings.133.34

ABSTRACT

The trial application of fibre optics and remote sensing techniques for monitoring a peanut-shaped tunnel boring machine (TBM) launching shaft in the Trunk Road T2 and Cha Kwo Ling Tunnel project has recently been completed. This is the first time in Hong Kong that these techniques are deployed to systematically monitor the entire excavation process of the peanut-shaped shaft. In particular, distributed fibre optic sensing (DFOS) technique based on optical frequency domain reflectometry (OFDR) was used to capture the continuous profiling of the strain measurement by fibre optics installed in the diaphragm wall panels, thus enabling the development of hoop strain to be revealed. To facilitate data interpretation, the excavation process was regularly recorded by the handheld light detection and ranging (LiDAR) scanning technique. This paper reports the background and key findings of the monitoring work as well as the results of the data analysis. The monitoring work provides valuable field data, which could not be easily obtained on site in the past. The data may be of use for numerical back-analysis to better understand the behaviour of shaft excavation. Insights gained in this study could also be useful to future design and construction of similar excavation works.

Keywords: Peanut-Shaped Excavation, Fibre Optics Monitoring, LiDAR scanning

1 Introduction

The use of circular excavation has become increasingly common for resisting the earth and groundwater pressures by mobilizing hoop compression. Pappin (2011) reported a series of case histories of circular excavations using diaphragm walls as earth retaining structure, including a case in Singapore using dual circular excavation, also known as “peanut-shaped” excavation. Similar peanut-shaped configuration as excavation support has been adopted in the Trunk Road T2 and Cha Kwo Ling Tunnel (collectively “the T2”) project in Hong Kong for the launching of the TBMs in order to enhance construction flexibility by eliminating steel struts, facilitate faster shaft excavation, assembly of the TBMs and construction of the permanent tunnel box structure, and significantly reduce impacts on adjacent structures and environment. However, the performance of such an innovative scheme, in particular the mobilisation of hoop action, has not been systematically monitored and reviewed in Hong Kong. Therefore, a comprehensive monitoring scheme was deployed to understand the performance of the peanut-shaped shaft excavation of the T2 project. Fibre optic sensing was proposed as the primary sensing technique for the monitoring scheme to monitor the structural performance of the shaft, supplemented by remote sensing technique using handheld LiDAR scanner to monitor the progression of excavation.

Various literature has reported a wide range of application of fibre optics on geotechnical engineering over the last decade such as the detection of slope and ground surface movements (e.g., Zhu et al. 2012, Kechavarzi et al. 2016 and Schenato et al. 2017), earth pressures measurements (e.g., Xu et al. 2017) and determination of soil nail forces (e.g., Zhu et al. 2012 and Kechavarzi et al. 2016).

Proceedings DOI: 10.21467/proceedings.133; Series: AIJR Proceedings; ISSN: 2582-3922; ISBN: 978-81-957605-1-0

Hoop action in circular excavation was studied by Schwamb et al. (2014) and Torisu et al. (2019) using distributed fibre optic sensing (DFOS) technique based on Brillouin optical time domain reflectometry (BOTDR) with a spatial resolution of 1.0 m. However, the behaviour of non-conventional circular shafts such as peanut-shaped excavation has not been studied in detail using such technology. In this study, the peanut-shaped shaft of the T2 project was instrumented with DFOS system based on optical frequency domain reflectometry (OFDR), which enables an improved spatial resolution of 5 cm.

Application of remote sensing techniques has also gained its popularity in geotechnical engineering over the last decade. In Hong Kong, the Geotechnical Engineering Office (GEO) of the Civil Engineering and Development Department (CEDD) has been applying various remote sensing techniques such as light detection and ranging (LiDAR), Interferometric Synthetic Aperture Radar (InSAR) and photogrammetry for acquisition of geospatial data to support geotechnical studies on landslide hazard. Amongst different techniques, LiDAR was considered the most effective for the unique terrain setting of Hong Kong (So et al. 2021). Comprehensive reviews on the application of different LiDAR equipment including terrestrial, airborne, mobile and handheld devices were given by Leung & Ho (2020). The use of handheld LiDAR scanner was found the most suitable for the remote, cramped and complicated site setting in Hong Kong due to its compactness, simple operation, and short mobilisation time while maintaining high accuracy. To date, most applications of handheld LiDAR devices were on slope stability and emergency landslide inspection. In this study, their application is extended to the monitoring of the excavation and lateral support works at the peanut-shaped shaft of the T2 project with an aim to assist the interpretation of fibre optics monitoring.

2 Project Background

The T2 project comprises 3.4 km of dual-two lane trunk road connecting the Central Kowloon Route on the West and the Tseung Kwan O-Lam Tin Tunnel on the East. Together they constitute Route 6. In this project, two 2.4 km sub-sea tunnels will be constructed mainly using two 14 m diameter TBMs drilling concurrently from Kai Tak through Kwun Tong Typhoon Shelter to Lam Tin. The TBM launching area comprised a conventional rectangular cut-and-cover tunnel and a peanut-shaped shaft as shown in Plate 1 and Figure 1. Both tunnel and shaft were constructed by diaphragm walls as vertical support elements. In this study, fibre optic cables were installed in three selected diaphragm wall panels as shown in Plate 1. Two panels, C1-01 and C2S-03 were located at the peanut-shaped shaft. The third panel, DN-03, was located at the cut-and-cover tunnel. As shown in Figure 1(b), the site is generally underlain by 14 m of fill and 5 m of marine deposits which overlaid 18 m of alluvium followed by 24 m of Completely Decomposed Granite (CDG) above the bedrock at around 60 m below ground. In general, the diaphragm wall panels in the cut-and-cover tunnel and the Y-shaped wall panels in the peanut-shaped shaft were founded on Grade III or better rock while the other panels in the peanut-shaped shaft were founded in CDG.

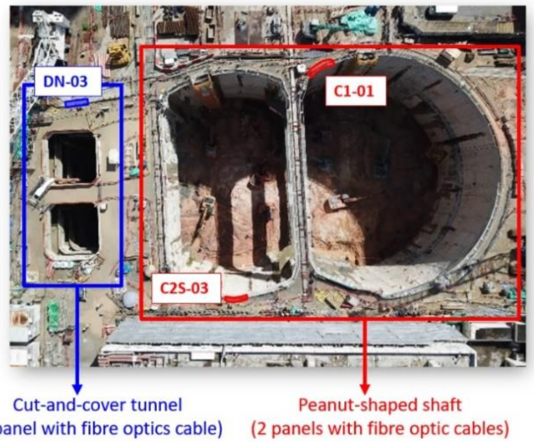

Plate 1: General view of the TBM launching area showing diaphragm wall panels with fibre optics cables instrumented

Proceedings DOI: 10.21467/proceedings.133
ISBN: 978-81-957605-1-0

Series: AIJR Proceedings
ISSN: 2582-3922

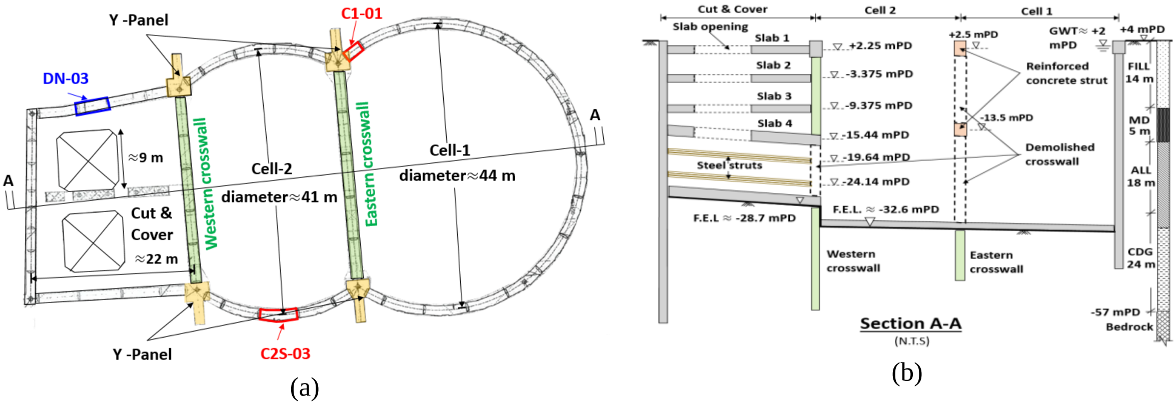

Figure 1: (a) General layout of the TBM launching area and (b) Cross section of the TBM launching area

The rectangular cut-and-cover tunnel was approximately 22 m long and 30 m wide on plan with a maximum excavation depth of about 32 m. The lateral support system included four layers of concrete slab and two layers of steel struts as shown in Figure 1(b). The peanut-shaped shaft was mainly constructed from two circular shafts, namely, "Cell 1" and "Cell 2", with diameters of approximately 44 m and 41 m respectively. The maximum excavation depth was approximately 38 m. Cell 1 and Cell 2 were connected by four Y-shaped wall panels and two crosswalls, namely, the eastern crosswall and western crosswall as shown in Figure 1(a). The peanut-shaped shaft was further supported laterally by two reinforced concrete beams installed at +2.5 mPD and -13.5 mPD spanning across the northern and southern side of the cofferdam as shown in Figure 1(b). The peanut-shaped cofferdam resisted the lateral earth and water pressure by developing compressive hoop forces which were then transferred to the Y-shaped wall panels, the reinforced beams and the two crosswalls.

The fibre optics and handheld LiDAR monitoring period was approximately 6 months, covering the pumping test, bulk excavation, lateral support and base slab installation works. It also captured the effect of the concurrent demolition of the crosswalls as the excavation proceeded. The construction sequence is mainly divided into six stages and they are plotted with the change in general excavation levels in the peanut-shaped shaft as shown in Figure 2.

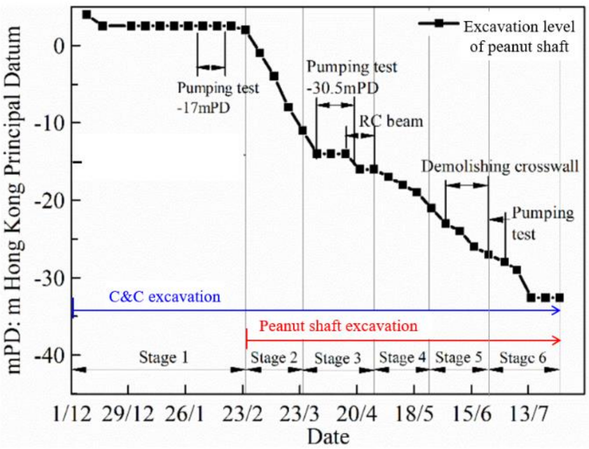

Figure 2: Construction sequence and general excavation levels in the peanut-shaped shaft

3 Distributed Fibre Optic Sensing (DFOS)

3.1 Working Principle

The basic working principle of using optical fibres for vibration, strain or temperature measurement is based on light scattering. Light, being a transverse electromagnetic wave, when being transmitted through the core of the optical fibre, interacts with the constituent atoms and molecules of the core.

Local impurities within the cable will cause back-scattering of the light (Soga & Luo 2018). If the fibre is subjected to temperature or strain changes, the characteristics of the back-scattered beam and thus the scattered signal in the fibre will be modulated by these physical changes. By measuring the changes of the modulated signal, the corresponding changes in strain and temperature can be correlated (Bao & Chen 2012). There are three different mechanisms of back-scattering – Rayleigh, Brillouin and Raman scattering as shown in the typical back-scattered light spectrum in Figure 3. A detailed account of different DFOS systems was given by Soga & Luo (2018), which are mainly catergorised based on the technique used for detection of various forms of back-scattering and hence the measurement of vibration, strain or temperature.

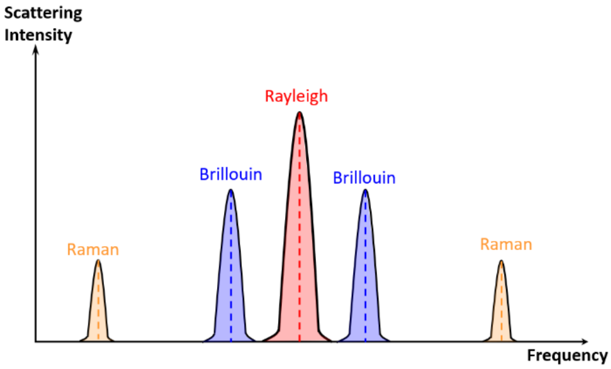

Figure 3: Typical spectrum showing three modes of back-scattering

In this study, the DFOS system adopted is based on optical frequency domain reflectometry (OFDR) for Rayleigh scattering detection. The typical set-up is shown in Figure 4. Similar set-up was also reported by Wu et al. (2020). The incident light from a tunable laser source is divided into the reference light and measurement light by an optical coupler. Once the measurement light is back-scattered, the back-scattered light will be mixed with the reference light by the optical coupler and subsequently demodulated by the photoelectric detector to obtain the strain and temperature measurement. The changes in strain and temperature can be correlated with the spectral shift by Equation (1):

$$\Delta v = C_{\varepsilon}\Delta\varepsilon + C_T\Delta T \quad \textbf{(1)}$$

where Δv = Rayleigh spectrum shift, $\Delta\varepsilon$ = strain changes in the fibre optic cable, ΔT = temperature change for the fibre optic cable, C_{ε} = strain change constant and C_T = temperature change constant

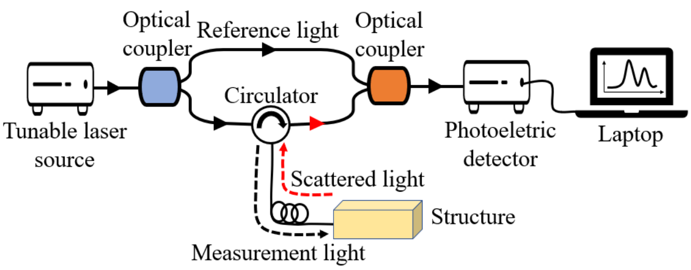

Figure 4: Typical set-up of OFDR for Rayleigh scattering detection

3.2 Field Installation and Monitoring

Two types of fibre optic cables, namely, strain sensing cable and temperature sensing cable, were installed in the three selected diaphragm wall panels for monitoring. The strain sensing cable is fabricated using tight-buffered, steel strand-reinforced and medium-density polyethylene (MDPE) with a diameter of 5.0 mm (Figure 5(a)). Strain is therefore transferred effectively due to the tight buffering while the cable is well protected by the steel strand reinforcement against damage during reinforcement cage transportation and tremie concreting. The temperature sensing cable is a loose tube cable of diameter of 5.0 mm. An annulus is maintained between the loose cable and the outer protective layer which comprises spiral armour, Kevlar, metal mesh and a low smoke halogen (LSZH) sleeve (Figure 5(b)). The annulus enables the loose cable to be free from mechanical strain and thus the strain changes due to temperature alone can be measured to compensate the strains measured by strain sensing cables.

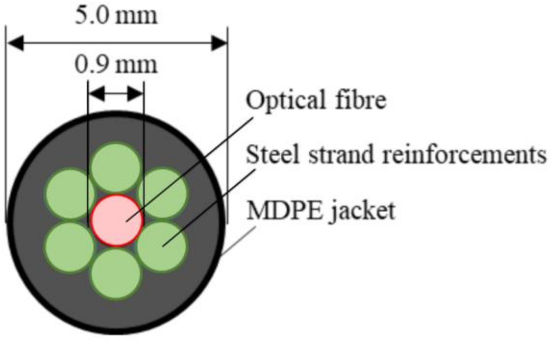

(a)

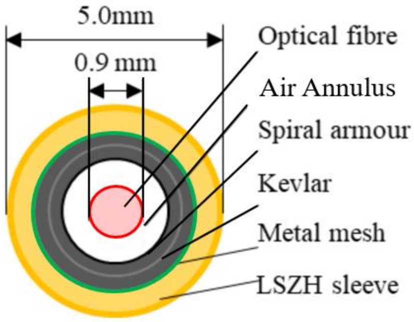

(b)

Figure 5: (a) Strain sensing cable and (b) temperature sensing cable

Strain and temperature sensing cables were installed on both the retained side and excavated side of the diaphragm wall panels. The typical arrangement of the cables is shown schematically in Figure 6(a). The strain sensing cables were arranged in two different configurations. One was aligned vertically along the wall panel for bending strain measurement for all three panels. The other was a zig-zag layout for hoop strain measurement at 6 different elevations (H1 to H6) for panels C1-01 and C2S-03. Meanwhile, temperature sensing cables were aligned vertically along all three wall panels to measure temperature induced strain at different elevations. The fixing details of the cables are shown in Figure 6(b). During the fabrication of the reinforcement cage, the cables were fixed to the steel bars of the reinforcement cage by hose clips and rubber sheets. Pre-tensioning was applied to both bending and hoop strain sensing cables using a tensioning device to achieve a pre-tensile strain of about 1000 $\mu\varepsilon$. Pre-tensioning enables easy identification of the measuring sections interested due to the exhibition of peak strain at the pre-tensioned sections of the cables (Schwamb et al. 2014). No pre-tensioning was applied to the temperature sensing cables. Due consideration and attention should also be given to the future construction activities near the instrumented panels. In panel C1-01, for instance, breaking of concrete cover was necessary as part of the construction to expose the couplers for connecting the lateral support beams. Based on experience gained, since the cables were placed very close to the concrete cover, extreme care must be exercised in installing cables and breaking concrete cover in panels of this type to avoid accidental exposure and physical damages to the cables.

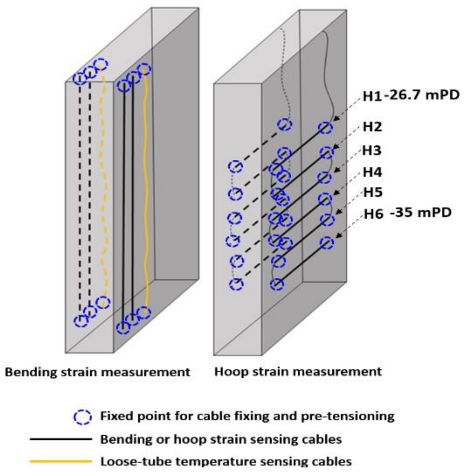

(a)

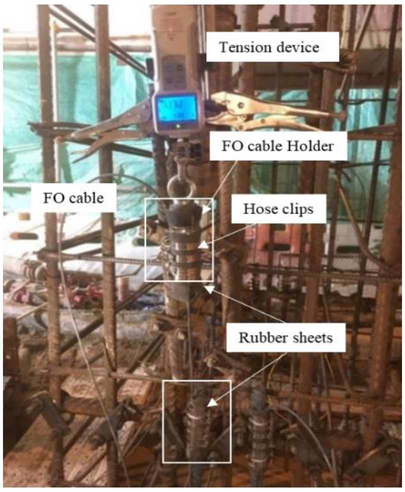

(b)

Figure 6: (a) Typical arrangement of fibre optic cables and (b) fixing details of fibre optic cables on reinforcement cages

DFOS data was collected using an OFDR-based interrogator (OSI-S). The device can produce a spatial resolution of 1 cm in a sensing range of 100 m with a measuring accuracy of $\pm 1\ \mu\varepsilon$. In this study, given the signal to noise ratio and the length of the fibre optic cables, a spatial resolution of 5 cm was achieved.

3.3 Data Analysis

3.3.1 Curvature and Lateral Wall Movement

Wall curvature can be computed from the strain measurement obtained from the retained side and excavated side using Equation (2):

$$k(z) = \frac{[\varepsilon_r(z) - \varepsilon_e(z)]}{\Delta d} \qquad \textbf{(2)}$$

where $k(z)$ = curvature at depth z, $\varepsilon_r(z)$ = strain at the retained side at depth z, $\varepsilon_e(z)$ = strain at the excavated side at depth z and Δd = horizontal distance between the cables on the retained side and the excavated side

Lateral wall deflection is then computed by double integration of the curvature obtained from Equation (2) above. Inclinometers were installed at or near the three instrumented wall panels for establishing the two boundary conditions for integration. The top deflection could therefore be derived directly from the measured top movement from inclinometer. The bottom deflection is taken as zero, which is the same assumption used for inclinometers.

The reliability of using fibre optic sensing to obtain wall curvature and deflection profile is best investigated using data obtained from wall panel no. DN-03 in the conventional multi-propped rectangular excavation, in which the results can be easily interpreted. Figure 7(a) and Figure 7(b) shows a comparison between the results obtained from inclinometers and fibre optic sensors on accumulative curvature and wall deflection of DN-03. The data shows the change from Stage 3 to Stage 5 where concurrent excavation and support installation took place in the rectangular tunnel. It can be seen that while the general trend of curvature was comparable between the two instruments, the fibre optic sensors registered a more reasonable curvature characteristic below the excavation depth with less fluctuation. Regarding wall deflection, a more consistent and comparable trend was observed. In particular, both optic fibre sensor and the inclinometer recorded a maximum deflection of about 28.4 mm and 37.2 mm respectively near the excavation depth at -25 mPD.

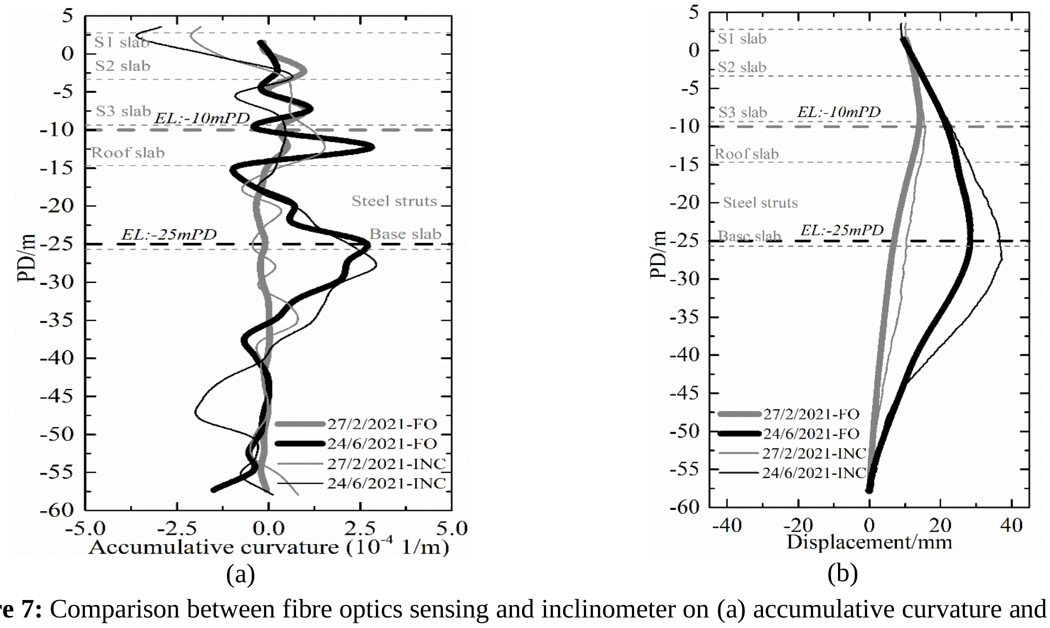

Figure 7: Comparison between fibre optics sensing and inclinometer on (a) accumulative curvature and (b) wall deflection on DN-03

3.3.2 Hoop Force and Circumferential Bending Moment

In this paper, the results from C2S-03 will be presented as an example to demonstrate the use of fibre optics sensing technology for studying hoop force and circumferential bending moment development in the peanut-shaped shaft. As mentioned in Section 3.2, hoop strains were measured at six different elevations from -26.7 mPD to -35 mPD across the wall panel indicated as H1 to H6. For better visualization, hoop strains from the top (H1), middle (H3) and bottom (H6) sections are presented as shown in Figure 8(a) and Figure 8(b) (tensile strain as positive and compressive strain as negative). The hoop strains indicated here were averaged out per 1 m cable length at each elevation and plotted against the construction stages Stage 1 (S1) to Stage 6 (S6). In general, both retained side and excavated side of the peanut-shaped shaft developed compressive hoop strain as the excavation works proceeded, with a larger hoop strain increase at the retained side, which is reasonable.

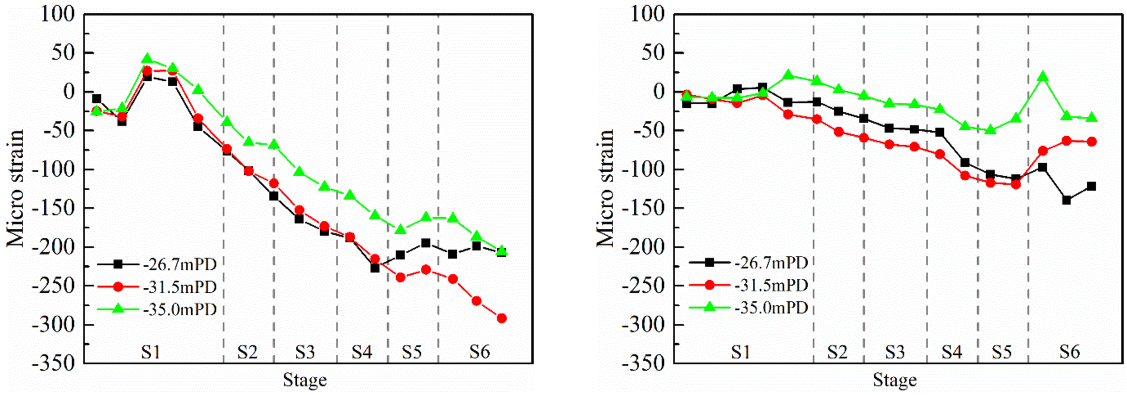

(a) (b)

Figure 8: (a) Hoop strains development on retained side and (b) hoop strains development on excavated side of C2S-03

To better understand the behaviour of the peanut-shaped excavation, the hoop force and circumferential bending moment of C2S-03 are presented in Figure 9(a) and Figure 9(b) respectively. During Stage 1, before excavation in Cell 1 and Cell 2, the positive hoop force and negative bending moment induced in C2S-03 were likely attributed by the partial lateral pressure release due to the excavation of the adjacent cut-and-cover tunnel. During Stage 2 to Stage 4, the combined effect of the dewatering and excavation works at the peanut-shaped shaft induced a progressive increase in compressive hoop force and hence an increase in circumferential bending moment. When the excavation level reached about -27 mPD at Stage 5, the western crosswall was concurrently demolished from -15.0 mPD to -25 mPD as shown in Figure 1(b). The release of the compressive hoop force and circumferential bending moment due to this crosswall demolition was successfully captured by the fibre optics sensors as highlighted in grey in Figure 9(a) and Figure 9(b). Once the excavation works proceeded beyond -25 mPD, both the compressive hoop force and circumferential bending moment increased again until they were generally stabilised when the final excavation level at about -32.6 mPD was reached during Stage 6.

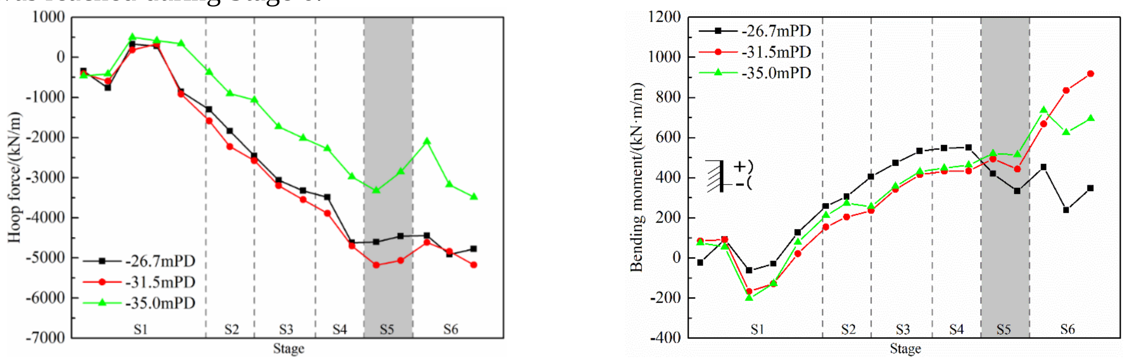

(a) (b)

Figure 9: (a) Hoop force development and (b) circumferential bending moment development of C2S-03

From the data analysis, it can be seen that DFOS technology offers an innovative and reliable solution in investigating the performance of the peanut-shaped excavation with partial crosswall demolition. In particular, the capability of producing continuous profiling of hoop forces and circumferential bending moment development is a clear advantage over other traditional instrumentations such as inclinometers and vibrating wire strain gauges, which only provide discrete measurement points.

4 Remote Sensing Using Handheld LiDAR Scanner

4.1 Methodology

Remote sensing using LiDAR technique was carried out as part of the monitoring scheme of the peanut-shaped excavation in the T2 project to obtain 3D geospatial information (point clouds) of the site. Given the cramped setting of the construction site with much plant and machinery that operated around the clock, handheld scanning devices were considered the most suitable where portability and efficiency were the main considerations such that impact to the construction progress could be minimised. In order to compare the 3D information with the actual site conditions and measurements, the point clouds obtained were transformed to the Hong Kong coordinate system HK80 by geo-referencing. A combination of fixed control points using existing structures coordinates and mobile control points using survey spheres was established on site to ensure sufficient control points could always be maintained within the line of sight throughout the monitoring period. In order to minimise cumulative error due to drift, a “closed loop” survey path was maintained in every scan to ensure the compounded error could be distributed within the loop. The scanning covered the entire TBM launching area at the T2 including both the cut-and-cover tunnel and peanut-shaped shaft.

4.2 Equipment and Data Acquisition

The portable scanning device adopted in this study was the ZEB Horizon. It mainly consists of a 2D laser range scanner head and a built-in inertial measurement unit (IMU) mounted on a rotary motor drive (Figure 10). The rotary action of the scanner provides the third dimension required to generate 3D information. The scanner head emits laser pulse and subsequently detects reflected pulses to determine the distance between the scanner and the objects being measured (Leung & Ho, 2020). Data received from the scanner head is then combined with the IMU data using the simultaneous localisation and mapping (SLAM) algorithm for acquisition of 3D point clouds (GeoSLAM Limited, 2020). The total weight including the battery and data-logger is only about 3 kg. The maximum scanning range is 100 m with a scanning rate of 300,000 points per second. A complete scan including set-up time required about 1.5 hour, which is considerably quicker than conventional land surveying, which normally takes at least half a day to cover a site of comparable size.

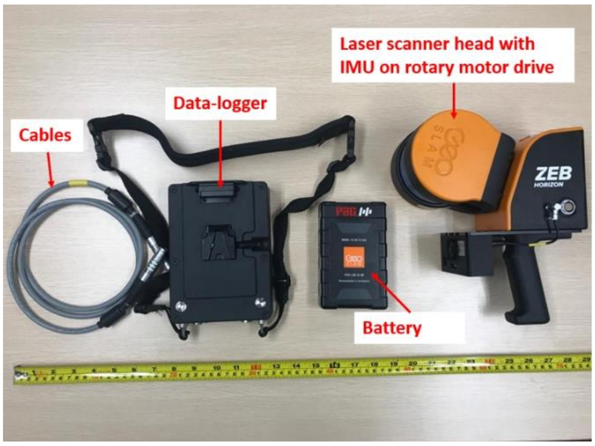

Figure 10: Main components of the handheld laser scanning device

4.3 Data Processing

The common data processing included noise removal, sub-sampling, geo-referencing and merging datasets, etc.

Noise was mainly contributed from moving objects, which generated redundant signal and should be removed.

In order to enhance the level of detail obtained from the cut-and-cover tunnel where multiple lateral supports were constructed, separate scanning was performed at close range at different support levels within the cut-and-cover tunnel. After geo-referencing, these individual sub-sample datasets could be easily merged to supplement the geospatial information of the main model. In this study, data processing was carried out using an open-source freeware CloudCompareV2 (CloudCompare 2015). Figure 11 shows the typical work flow outlining the processing tasks to produce a 3D model of the TBM launching area.

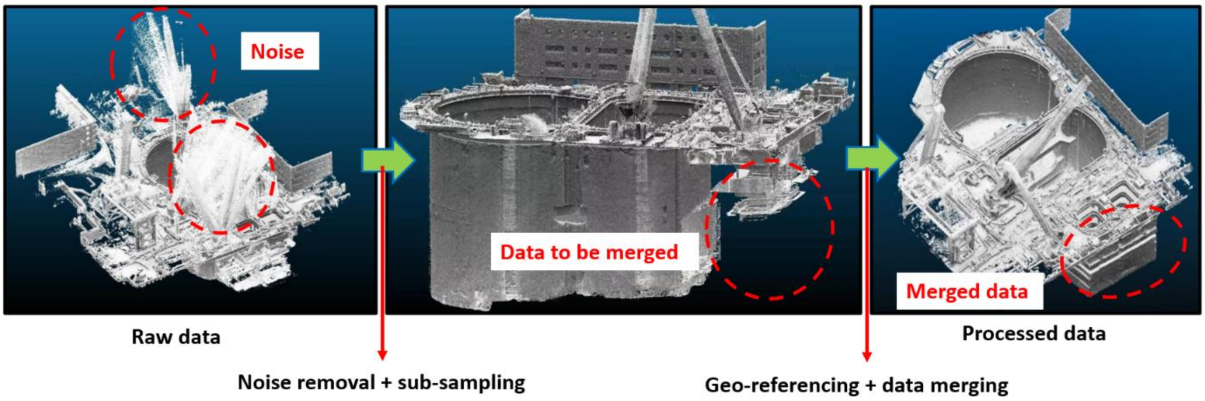

Figure 11: Typical workflow of data processing

4.4 Data Analysis

The processed data, being geo-referenced, enable useful analysis like cutting cross-sections, dimension measurement and estimation of excavation extent, etc. By way of an example, Figure 12(a) shows the measurement of excavation depth of a typical cross-section extracted from the cofferdam using CloudCompareV2. Throughout the construction, a trial location was selected and a comparison was made between LiDAR measurement and site records on excavation level as plotted in Figure 12(b). It demonstrates that LiDAR measurement can provide reasonably comparable results. The use of LiDAR technique offers an added advantage of capturing the entire profile in the space as compared with integrating single measurement points manually based on the conventional survey method.

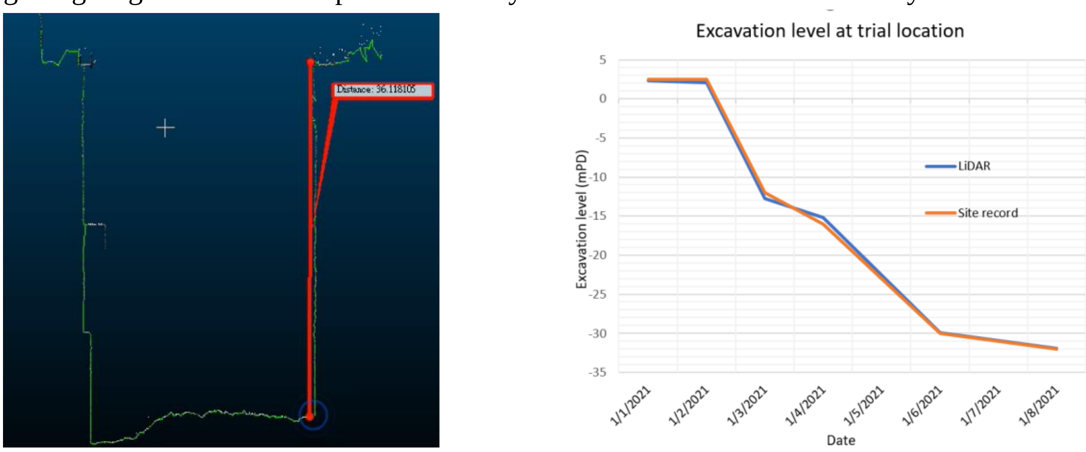

(a) (b)

Figure 12: (a) Typical cross section extracted from 3D LiDAR model and (b) comparison between LiDAR measurement and site measurement

Previous LiDAR studies undertaken on natural hillsides or landslide sites seldom involved frequent and periodic scanning. Their data analysis was largely based on a single model. Change detection application reported by So et al. (2021) was based on 3 different LiDAR datasets that were few to ten years apart for assessing change of ground profile due to landslide. However, a higher monitoring frequency is more suitable for excavation and lateral support works. In this study, frequent scanning on a weekly basis was carried out throughout the entire monitoring period. Over 30 complete datasets were acquired. The geo-referenced 3D information can be integrated against time for a complete 3D visualisation of the construction sequence. Figure 13 shows some extracted dataset which are correlated with the construction sequence Stage 1 to Stage 6 mentioned in Figure 2.

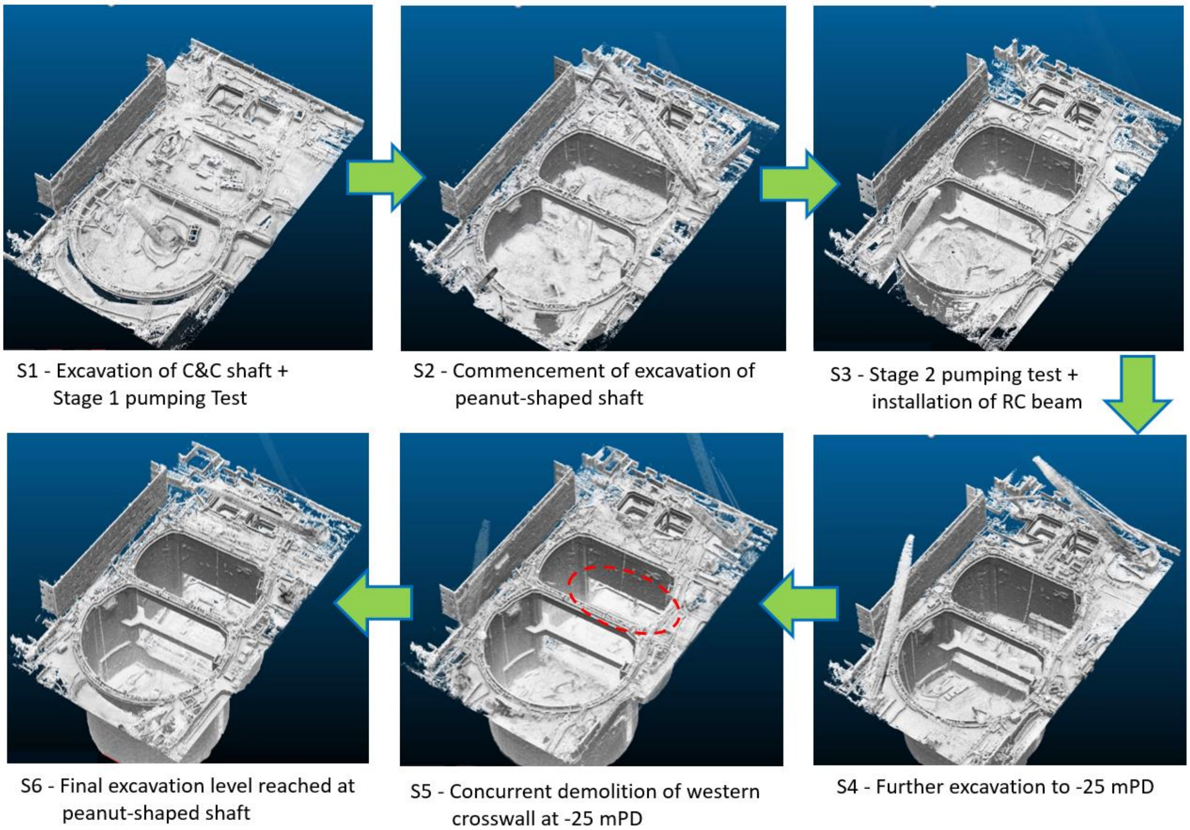

Figure 13: 3D visualisation of construction sequence from LiDAR dataset showing key construction stages S1 to S6

Given the complex site setting and construction sequence of the T2 project, the 3D construction sequence visualisation served as a useful tool for prompt cross-checking of the actual construction progress against the design scheme. The LiDAR data successfully captured the critical activities such as excavation, installation of lateral supports and crosswall demolition. Clearly, the information obtained further reinforced the interpretation of the fibre optics results presented in Section 3 above.

5 Conclusions

This paper presented the state-of-the-art monitoring techniques employing fibre optics sensing and handheld remote sensing devices using LiDAR to study the behaviour of a peanut-shaped excavation, which is first of its kind being implemented in Hong Kong. Fibre optics sensing offers superior capability over traditional monitoring instruments in terms of producing continuous profiling of hoop strains, hoop forces and circumferential bending moment, which are essential in assessing the soil-structure interaction of non-conventional circular excavation. Wall deflection profiles obtained are comparable with those obtained from inclinometers. Potential further work including using the fibre

Proceedings DOI: 10.21467/proceedings.133
ISBN: 978-81-957605-1-0

Series: AIJR Proceedings
ISSN: 2582-3922

optics data for numerical back-analysis can be explored to facilitate the future design and construction of excavation and lateral support works of a similar nature. The simple operation of handheld LiDAR scanner also greatly reduces the surveying time and minimises disturbance to the site works. Digitisation of actual site conditions allows quick data analysis to assist the verification of design and monitoring of construction progress. Further application is envisaged to incorporate the 3D dataset into the Building Information Modelling (BIM) system to facilitate design optimisation and assets management.

6 Declarations

6.1 Acknowledgements

This paper is published with the permission of the Director of Civil Engineering and Development, the Head of the Geotechnical Engineering Office, the Project Manager of the East Development Office and the Hong Kong Polytechnic University of the Hong Kong Special Administrative Region, China.

6.2 Publisher's Note

AIJR remains neutral with regard to jurisdictional claims in published maps and institutional affiliations.

References

Bao, X. & Chen, L. 2012. Recent progress in distributed fiber optic sensors. Sensors 2012, 12(7): 8601-8639.

CloudCompare 2015. CloudCompare Version 2.6.1: User Manual. CloudComapre.

GeoSLAM Limited. 2020. ZEB-Horizon User's Manual v1.3. GeoSLAM Limited.

Kechavarzi, C., Soga, K., de Battista, N., Pelecanos, L., Elshafie, M.Z.E.B. & Mair, R.J. 2016. Distributed Fibre Optic Strain Sensing for Monitoring Civil Infrastructure-A practical guide. ICE Publishing.

Leung, W.K. & Ho, Y.K. 2020. A New Generation of Handheld Laser Scanning for Quality Enhancement in Geotechnical Studies. Proceedings of HKIE Geotechnical Division Annual Seminar 2020: 50-61.

Pappin, J.W. 2011. Circular excavations using diaphragm walls. APEC Seminar on the State-of-the-Practice of Deep Excavation Works in Malaysia, Taiwan and Hong Kong 2011: 111-120.

Schenato, L., Palmieri, L., Camporese, M., Bersan, S., Cola, S., Pasuto, A., Galtarossa, A., Salandin, P. & Simonini, P. 2017. Distributed optical fibre sensing for early detection of shallow landslides triggering. Scientific Reports 7: 14686. DOI: 10.1038/s41598- 017-12610-1.

Schwamb, T., Soga, K., Mair, R. J., Elshafie, M.Z.E.B., Sutherden, R., Boquet, C., & Greenwood, J. 2014. Fibre optic monitoring of a deep circular excavation. Proceedings of the Institution of Civil Engineers - Geotechnical Engineering, 167(2): 144-154. ICE Publishing.

So, A.C.T., Ho, T.Y.K., Wong, J.C.F., Lai, A.C.S., Leung, W.K. & Kwan, J.S.H. 2021. Advancing the use of LiDAR in geotechnical applications in Hong Kong – A 10-year overview. The 42nd Asian Conference on Remote Sensing (ACRS2021), Vietnam, 22-24 November 2021: pp 11.

Soga, K. & Luo, L. 2018. Distributed fiber optics sensors for civil engineering infrastructure sensing. Journal of Structural Integrity and Maintenance, 3(1): pp 21.

Torisu, S.S., Faustin, N.E., Elshafie, M.Z.E.B., Black, M., Soga, K., & Mair, R.J. 2019. Monitoring of Shaft Excavations in Clay. International Conference on Smart Infrastructure and Construction 2019 (ICSIC): 655-664. ICE Publishing.

Wu, H., Zhu, H.H., Zhang, C.C., Zhou, G.Y., Zhu, B., Zhang, W. & Azarafza, M. 2020. Strain integration-based soil shear displacement measurement using high-resolution strain sensing technology. Measurement, 166: pp 12.

Xu, D.S., Dong, L.J., Borana, L. & Liu, H.B. 2017. Early-warning system with quasi-distributed fiber optic sensor networks and cloud computing for soil slopes. IEEE Access, vol. 5: 25437 – 25444. DOI: 10.1109/ACCESS.2017.2771494.

Zhu, H.H., Ho, A.N.L., Yin, J.H., Sun, H.W., Pei, H.F. & Hong, C.Y. 2012. An optical fibre monitoring system for evaluating the performance of a soil nailed slope. Smart Structures and Systems 9(5): 393-410.